Injective Shape Deformations Using Cube-Like Cages

Jiri Kosinka[1] and Michael Barton[2]

[1]University of Oslo, jiri.kosinka@cma.uio.no
[2]Technion, barton@cs.technion.ac.il

ABSTRACT

The present paper investigates an application of Warren's coordinates for convex polytopes to space deformations. We show that the use of cube-like cages presents a good compromise between the degrees of freedom of the deformation and the complexity of the mapping itself. As our main result we give simple sufficient conditions on injectivity of deformations based on cube-like cages.

1   INTRODUCTION

Barycentric coordinates play a very important role in computer graphics and applications, e.g. shading, planar and spatial deformations, animations, etc. One of the most widely used coordinates are the mean-value coordinates [3]. These coordinates are positive over convex polygons and can be generalized to non-convex polygons [8] and to R^3 [2,4]. Another set of coordinates for convex polygons are the Wachspress coordinates [12]. However, they do not generalize in a natural way to non-convex polygons. One of possible generalizations of Wachspress coordinates to higher dimensions was introduced in [13] and later studied in [9] - the so called Warren's coordinates. Other methods using barycentric coordinates include [11] and [14].

On the other hand, numerous techniques for shape deformations not based on barycentric coordinates were designed, see the survey [6] and the references cited therein. The so-called free form deformations are widely used in applications. However, there are only few known deformation techniques that are guaranteed to be fold-over free, cf. Table 1 of [6]. The injectivity of free form deformations was studied in [7].

Injectivity of barycentric mappings and other types of planar and spatial deformation has not been studied widely in the literature. The mapping induced by mean-value coordinates fails to be injective in some extreme cases [5]. On the other hand, Wachspress coordinates [12] give rise to injective mappings between convex polygons [5].

In the present paper we investigate an application of Warren's coordinates [13] to space deformations that they induce. In general, these coordinates are defined for convex polytopes. We restrict ourselves to cube-like polyhedra only. Indeed, too many degrees of freedom, represented by control points, might become overwhelming for an inexperienced user. We show that this special, simple subclass of polyhedra gives rise to cage deformations with sufficiently many degrees of

freedom. Moreover, we give a set of linear conditions that guarantee injectivity of these deformations. Due to its simplicity, the user can be provided with an interactive feedback on the injectivity of the deformation. This new set of *sufficient* conditions on injectivity also allows a nice geometric interpretation.

The remainder of the paper is organized as follows. The next section describes feasible cube-like cages that can be used for shape deformations using Warren's coordinates. Section 3 recalls Warren's coordinates and barycentric mappings induced by them. In Section 4 we discuss conditions on injectivity of barycentric mappings. Section 5 then applies these results to space deformations using cube-like cages. Finally, the paper is concluded with several examples and a discussion of future work.

2   CUBE-LIKE CAGES

Consider the unit cube U with vertices

$$\boldsymbol{u}_1 = (1,0,0), \boldsymbol{u}_2 = (1,1,0), \boldsymbol{u}_3 = (0,1,0), \boldsymbol{u}_4 = (0,0,0), \boldsymbol{u}_5 = (1,0,1), \boldsymbol{u}_6 = (1,1,1), \boldsymbol{u}_7 = (0,1,1), \boldsymbol{u}_8 = (0,0,1). \quad (2.1)$$

U is considered as an open set in R^3. Its closure will be denoted $\overline{U}$ and its boundary ∂U. Let $P \subset R^3$ be a cage (closed mesh) with vertices $\boldsymbol{p}_1, \boldsymbol{p}_2 ..., \boldsymbol{p}_8$ which is combinatorially equivalent to the cage associated with U, i.e., there is a one-to-one correspondence between the vertices and edges of U and P. Denote $F_1, ..., F_6$ the 6 faces of U. If $\boldsymbol{u}_i, \boldsymbol{u}_j, \boldsymbol{u}_k$ and $\boldsymbol{u}_l$ belong to $F_m, m = 1, ..., 6$ then we denote G_m the tetrahedron (or planar quadrilateral) formed by $\boldsymbol{p}_i, \boldsymbol{p}_j, \boldsymbol{p}_k$ and $\boldsymbol{p}_l$. Moreover, let $Int_g(G)$ denote the *geometric interior* of G. If G is a tetrahedron then $Int_g(G)$ is the interior of G in R^3. If G is a planar quadrilateral lying in a plane π, then $Int_g(G)$ is the interior of G in π (the usual $Int(G)$ in R^3 is the empty set in this quadrilateral case).

Definition 2.1: Let $Int_g(G_i) \cap Int_g(G_j) = \varnothing$ for all $i, j = 1, ..., 6, i \neq j$. Then P is called a *cube-like cage*.

As an example of a cube-like cage, P can be chosen to form an affine image (parallelepiped) or a projective image of a cube, where no point of the cube is mapped to infinity. However, cube-like cages are more general since its 'faces' G_m are not required to be planar, see Section 6 for examples.

We will focus on deformations based on a set of barycentric coordinates defined in [13]. Since these coordinates are well defined for convex polytopes only, we assume that P is a *convex* cube-like cage with all its 'faces' G_m *planar* for the remainder of the paper. Moreover, P will be said to form a *cube-like convex polyhedron*.

Since the coordinates of Warren [13] are invariant with respect to affine transforms, we can assume, without loss of generality, that

$$\boldsymbol{p}_1 = (1,0,0), \boldsymbol{p}_2 = (x_2, y_2, 0), \boldsymbol{p}_3 = (0,1,0), \boldsymbol{p}_4 = (0,0,0), \boldsymbol{p}_5 = (x_5, 0, z_5), \boldsymbol{p}_6 = (x_6, y_6, z_6), \boldsymbol{p}_7 = (0, y_7, z_7), \boldsymbol{p}_8 = (0,0,1). \quad (2.2)$$

We denote by $V(\boldsymbol{p}, \boldsymbol{q}, \boldsymbol{r}, \boldsymbol{s})$ the signed volume of the tetrahedron $[\boldsymbol{p}, \boldsymbol{q}, \boldsymbol{r}, \boldsymbol{s}]$,

$$V(\boldsymbol{p}, \boldsymbol{q}, \boldsymbol{r}, \boldsymbol{s}) = \frac{1}{6} \begin{vmatrix} 1 & 1 & 1 & 1 \\ p^1 & q^1 & r^1 & s^1 \\ p^2 & q^2 & r^2 & s^2 \\ p^3 & q^3 & r^3 & s^3 \end{vmatrix} . \quad (2.3)$$

Since *P* must have planar faces, we obtain that

$$
\begin{aligned}
V(\boldsymbol{p}_5, \boldsymbol{p}_6, \boldsymbol{p}_7, \boldsymbol{p}_8) &= x_6 y_7 - x_5 y_7 + x_5 y_6 - x_5 y_6 z_7 + x_5 z_6 y_7 - z_5 x_6 y_7 = 0, \\
V(\boldsymbol{p}_2, \boldsymbol{p}_3, \boldsymbol{p}_7, \boldsymbol{p}_6) &= x_6 z_7 - x_2 z_6 y_7 + x_2 y_6 z_7 + x_2 z_6 - x_2 z_7 - y_2 x_6 z_7 = 0, \\
V(\boldsymbol{p}_1, \boldsymbol{p}_2, \boldsymbol{p}_6, \boldsymbol{p}_5) &= x_2 y_6 z_5 - y_2 x_6 z_5 + y_2 x_5 z_6 - y_6 z_5 + y_2 z_5 - y_2 z_6 = 0
\end{aligned}
\tag{2.4}
$$

must hold. This gives a system of 3 linear equations in x_6, y_6, z_6. A thorough description of all feasible cages falls beyond the scope of the present paper. Therefore, we restrict ourselves to a brief description only. In general, one can choose the free parameters $x_2, y_2, x_5, z_5, x_7, z_7$ and compute unique x_6, y_6, z_6 from Eqn. (2.4). Moreover, since the faces of *P* must be convex, we obtain a system of linear inequalities. However, all the linear constraints can be satisfied easily and *P* can be interactively created and modified to become a cube-like convex polyhedron. See Section 6 for examples of feasible cages *P*.

Whereas cages based on affine and projective images of a cube offer 12 and 15 degrees of freedom (DOF), respectively, a cube-like cage admits 18 DOFs. More precisely, in the case of parallelepipeds, the cage is uniquely determined by an affine image of a simplex, which gives 3 x 4 = 12 DOFs. Using projective transformations, one can fix a geometric basis of points in 3D, i.e., 5 points, yielding 15 DOFs. Finally, since we have 8 free vertices and 6 volumetric constraints, the case of a cube-like convex polyhedron admits 3 x 8 - 6 = 18 DOFs.

3 BARYCENTRIC MAPPINGS

We make use of the dual construction proposed in [9]. For the convenience of the reader we recall the essential parts of the approach taken therein.

Let $\boldsymbol{p}_i$ be a vertex of *P*. Note that all vertices of *P* are of valence 3. Let $\boldsymbol{n}_{i,1}, \boldsymbol{n}_{i,2}, \boldsymbol{n}_{i,3}$ be the outward normals of the 3 faces containing $\boldsymbol{p}_i$. Since the dual vertices have the form $\boldsymbol{n}_{i,\alpha} / \boldsymbol{n}_{i,\alpha} \cdot (\boldsymbol{p}_i - \boldsymbol{x})$, see [9], the weight w_i associated to vertex $\boldsymbol{p}_i$ is given by the unsigned volume

$$
w_i = 3V\left(0, \frac{\boldsymbol{n}_{i,1}}{\boldsymbol{n}_{i,1} \cdot (\boldsymbol{p}_i - \boldsymbol{x})}, \frac{\boldsymbol{n}_{i,2}}{\boldsymbol{n}_{i,2} \cdot (\boldsymbol{p}_i - \boldsymbol{x})}, \frac{\boldsymbol{n}_{i,3}}{\boldsymbol{n}_{i,3} \cdot (\boldsymbol{p}_i - \boldsymbol{x})}\right).
\tag{3.1}
$$

Now, denoting $\mu = \sum_{i=1}^{8} w_i$, the barycentric coordinate associated to $\boldsymbol{p}_i$ is given by $\lambda = \frac{w_i}{\mu}$. Then the set $\{\lambda_i, i = 1, \ldots, 8\}$ is called the set of *Warren's coordinates* for *P*. We remark that for the unit cube *U* Warren's coordinates reduce to

$$
\begin{aligned}
\lambda_1 &= x(1-y)(1-z), \lambda_2 = xy(1-z), \lambda_3 = (1-x)y(1-z), \lambda_4 = (1-x)(1-y)(1-z), \\
\lambda_5 &= x(1-y)z, \lambda_6 = xyz, \lambda_7 = (1-x)yz, \lambda_8 = (1-x)(1-y)z.
\end{aligned}
\tag{3.2}
$$

Warren's coordinates, as all barycentric coordinates, satisfy the following properties:

$$
\lambda_i \geq 0, \qquad \boldsymbol{x} \in \overline{P},
$$

$$
\sum_{i=1}^{8} \lambda_i(\boldsymbol{x}) = 1, \qquad \boldsymbol{x} \in \overline{P},
\tag{3.3}
$$

$$
\sum_{i=1}^{8} \lambda_i(\boldsymbol{x}) \boldsymbol{p}_i = \boldsymbol{x}, \qquad \boldsymbol{x} \in \overline{P}.
$$

In other words, they are *non-negative* and satisfy the *partition of unity* and *barycentric property*. Moreover, the *Lagrange property* holds as well, i.e., $\lambda_i(\boldsymbol{p}_j) = \delta_{ij}$.

Let Q be a second cube-like cage. Using Warren's coordinates, we define the mapping

$$\boldsymbol{f}(\boldsymbol{x}) = \sum_{i=1}^{8} \lambda_i(\boldsymbol{x})\boldsymbol{q}_i = \boldsymbol{x}, \qquad \boldsymbol{x} \in P. \tag{3.4}$$

Remark 3.1: As it was observed in [13], the mapping $\boldsymbol{f}$ restricted to faces (edges) of P acts as Warren's mapping for one (two) dimensions lower. Thus, $\boldsymbol{f}$ extends continuously to ∂P and therefore it is well defined in ∂P.

From the properties of λ_i we see that the mapping $\boldsymbol{f}$ is a convex-combination mapping. Therefore, the point $\boldsymbol{f}(\boldsymbol{x})$ must belong to the convex hull of $\bar{Q}$. Moreover, using the Lagrange property of λ_i it follows that $\boldsymbol{f}(\boldsymbol{p}_i) = \boldsymbol{q}_i$.

We emphasize that Q is not required to form a convex polyhedron for the mapping $\boldsymbol{f}$ to be well defined. Therefore, the mapping $\boldsymbol{f}$ is more general than affine and even projective mappings (restricted to $\bar{P}$ and when no point of $\bar{P}$ is mapped to infinity). Nevertheless, in order for $\boldsymbol{f}$ to be usable in practice for shape deformations and other applications, it is often required that $\boldsymbol{f}$ be injective. This gives us a guarantee that $\boldsymbol{f}$ does not introduce any new self-intersections in the deformed shape.

4   CONDITIONS ON INJECTIVITY

Following Remark 3.1, faces of P, forming convex quadrilaterals, are mapped to Wachspress interpolants (see [12]). Edges of P are mapped in a linear fashion, i.e., an edge of P given by $\boldsymbol{p}_i, \boldsymbol{p}_j$ is mapped onto the line segment determined by $\boldsymbol{q}_i, \boldsymbol{q}_j$. Turning to the results of [5] we conclude that $\boldsymbol{f}$ is injective in ∂P.

Since $\boldsymbol{f}$ *is* C^∞ in P, $\boldsymbol{f}$ continuously extends to ∂P and $\boldsymbol{f}$ is injective in ∂P, the question of injectivity of $\boldsymbol{f}$ reduces to whether its Jacobian does not change sign in P, see e.g. [10]. If $\boldsymbol{f}(\boldsymbol{x}) = (f(\boldsymbol{x}), g(\boldsymbol{x}), h(\boldsymbol{x}))$ and $\partial_r h(\boldsymbol{x}) = \partial h / \partial \boldsymbol{x}^r, r = 1, 2, 3,$ the Jacobian of $\boldsymbol{f}$ is the determinant

$$J(\boldsymbol{f}) = \begin{vmatrix} \partial_1 f & \partial_1 g & \partial_1 h \\ \partial_2 f & \partial_2 g & \partial_2 h \\ \partial_3 f & \partial_3 g & \partial_3 h \end{vmatrix}. \tag{4.1}$$

Similarly to the planar case, cf. Lemma 1 of [5], the following lemma can be proved using the matrix identity

$$\begin{pmatrix} 1 & f & g & h \\ 0 & \partial_1 f & \partial_1 g & \partial_1 h \\ 0 & \partial_2 f & \partial_2 g & \partial_2 h \\ 0 & \partial_3 f & \partial_3 g & \partial_3 h \end{pmatrix} = \begin{pmatrix} \lambda_1 & \cdots & \cdots & \lambda_8 \\ \partial_1 \lambda_1 & \cdots & \cdots & \partial_1 \lambda_8 \\ \partial_2 \lambda_1 & \cdots & \cdots & \partial_2 \lambda_8 \\ \partial_3 \lambda_1 & \cdots & \cdots & \partial_3 \lambda_8 \end{pmatrix} \begin{pmatrix} 1 & q_1^1 & q_1^2 & q_1^3 \\ \vdots & \vdots & \vdots & \vdots \\ \vdots & \vdots & \vdots & \vdots \\ 1 & q_8^1 & q_8^2 & q_8^3 \end{pmatrix} \tag{4.2}$$

and applying the Cauchy-Binet theorem (see formula (1.23) of [1]) to it.

Lemma 4.1: For any set of differentiable functions $\lambda_1,...,\lambda_8$ satisfying the partition of unity,

$$J(\boldsymbol{f})(\boldsymbol{x}) = 6 \sum_{1 \le i < j < k < l \le 8} D(\lambda_i, \lambda_j, \lambda_k, \lambda_l)(\boldsymbol{x})\, V(\boldsymbol{q}_i, \boldsymbol{q}_j, \boldsymbol{q}_k, \boldsymbol{q}_l), \tag{4.3}$$

where

$$D(a,b,c,d) = \begin{vmatrix} a & b & c & d \\ \partial_1 a & \partial_1 b & \partial_1 c & \partial_1 d \\ \partial_2 a & \partial_2 b & \partial_2 c & \partial_2 d \\ \partial_3 a & \partial_3 b & \partial_3 c & \partial_3 d \end{vmatrix}. \tag{4.4}$$

The following lemma simplifies our further computations.

Lemma 4.2: For differentiable functions a, b, c, d and $\nu > 0$

$$D(\nu a, \nu b, \nu c, \nu d) = \nu^4 D(a,b,c,d). \tag{4.5}$$

The proof is similar to the one of Lemma 2 of [5]. Using Lemma 4.1 and setting $\nu = 1/\mu$ in Lemma 4.2 we obtain the following sufficient conditions for the injectivity of the mapping f.

Theorem 4.3: Let for all $\boldsymbol{x} \in P$

$$D(\lambda_i, \lambda_j, \lambda_k, \lambda_l)(\boldsymbol{x})\, V(\boldsymbol{q}_i, \boldsymbol{q}_j, \boldsymbol{q}_k, \boldsymbol{q}_l) > 0 \tag{4.6}$$

for all $1 \le i < j < k < l \le 8$ or

$$D(\lambda_i, \lambda_j, \lambda_k, \lambda_l)(\boldsymbol{x})\, V(\boldsymbol{q}_i, \boldsymbol{q}_j, \boldsymbol{q}_k, \boldsymbol{q}_l) < 0 \tag{4.7}$$

for all $1 \le i < j < k < l \le 8$. Then the mapping f given by Eqn. (3.4) is injective.

5   INJECTIVE DEFORMATIONS

Following Theorem 4.3 and Lemma 4.1 we investigate the quantity $D(w_i, w_j, w_k, w_l)(\boldsymbol{x})$. Since we need to consider indices satisfying $1 \le i < j < k < l \le 8$, it would be necessary to check 70 terms in a concrete example. However, a long and tedious computation (with the help of a suitable computer algebra system) reveals that for a cube-like convex polyhedron the terms $D(\lambda_i, \lambda_j, \lambda_k, \lambda_l)(\boldsymbol{x})$ simplify significantly.

Lemma 5.1: For all $\boldsymbol{x} \in P$ and for all $1 \le i < j < k < l \le 8$ it holds

$$D(w_i, w_j, w_k, w_l) = 12 w_i w_j w_k w_l \mu\; V(\boldsymbol{u}_i, \boldsymbol{u}_j, \boldsymbol{u}_k, \boldsymbol{u}_l). \tag{5.1}$$

Since all w_i and μ are positive in P and at least some $V(\boldsymbol{u}_i, \boldsymbol{u}_j, \boldsymbol{u}_k, \boldsymbol{u}_l)$ are non-zero, combining this result with Lemma 4.1 and Theorem 4.3 we have proved the following

Theorem 5.2: Let P form a cube-like convex polyhedron and Q be cube-like. Let

$$V(\boldsymbol{u}_i, \boldsymbol{u}_j, \boldsymbol{u}_k, \boldsymbol{u}_l)\; V(\boldsymbol{q}_i, \boldsymbol{q}_j, \boldsymbol{q}_k, \boldsymbol{q}_l) \ge 0 \tag{5.2}$$

for all $1 \leq i < j < k < l \leq 8$ or

$$V(\boldsymbol{u}_i, \boldsymbol{u}_j, \boldsymbol{u}_k, \boldsymbol{u}_l) \; V(\boldsymbol{q}_i, \boldsymbol{q}_j, \boldsymbol{q}_k, \boldsymbol{q}_l) \leq 0 \tag{5.3}$$

for all $1 \leq i < j < k < l \leq 8$. Then the mapping f given by Eqn. (3.4) is injective.

Eqn. (5.2), resp. (5.3), gives $\begin{pmatrix} 8 \\ 4 \end{pmatrix} = 70$ conditions. However, as U is a cube, 12 of the conditions are equal to zero as 12 of the volumes $V(\boldsymbol{p}_i, \boldsymbol{p}_j, \boldsymbol{p}_k, \boldsymbol{p}_l)$ vanish. Therefore, one can extract 58 inequalities from Eqn. (5.2), resp. (5.3), which form a set of sufficient conditions for the barycentric mapping f to be injective.

Consequently, to the best of our knowledge we believe that the conditions in Theorem 5.2 are the simplest sufficient conditions known. Also, they are the most useful ones since they provide a nice geometric insight into the problem by relating the volumes $V(\boldsymbol{u}_i, \boldsymbol{u}_j, \boldsymbol{u}_k, \boldsymbol{u}_l)$ associated to U with the volumes $V(\boldsymbol{q}_i, \boldsymbol{q}_j, \boldsymbol{q}_k, \boldsymbol{q}_l)$ associated to Q.

Once a given shape is enclosed by a cube-like convex polyhedron P (with 18 DOFs, see Section 2), the user is provided with 8 vertices (24 DOFs) for controlling the deformation f. By moving one of the vertices, the given shape is deformed accordingly. If a fold-over free deformation is required, one can simply test the sufficient conditions given in Theorem 5.2. Finally, we emphasize that these sufficient conditions are linear in the vertices of Q and *constant* in x. This fact makes them suitable for applications such as interactive shape deformation since they can be easily evaluated and tested in real-time.

6   EXAMPLES

In this section we present several examples of shape deformations. All examples were created using the GuIrit GUI user interface (www.cs.technion.ac.il/~gershon/GuIrit) of the Irit solid modeling system (www.cs.technion.ac.il/~irit).
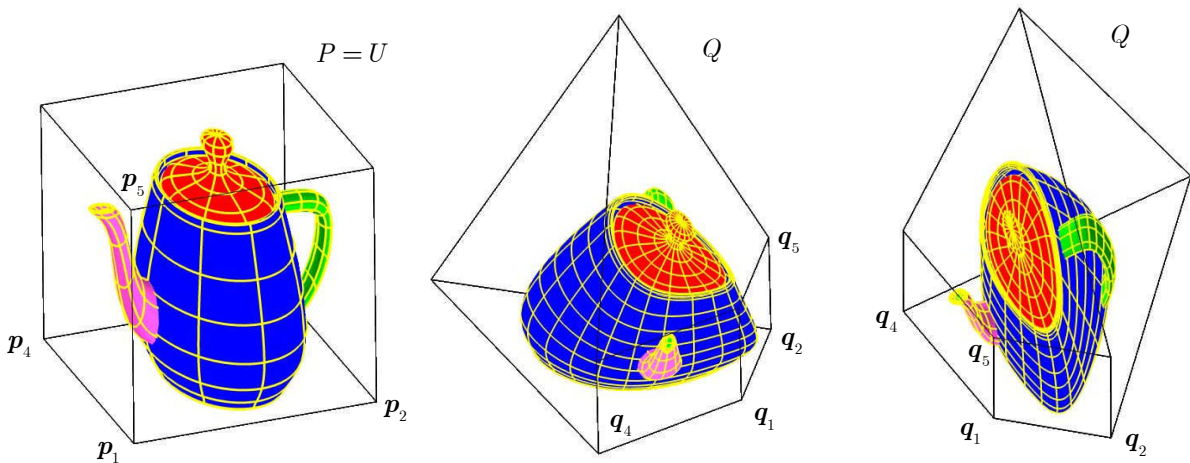

Fig. 1: Warren's mapping is reduced to trilinear mapping for $P = U$. The injectivity of the mapping is guaranteed by checking only the signs of volumes of all corresponding tetrahedrons, i.e $V(\boldsymbol{p}_i, \boldsymbol{p}_j, \boldsymbol{p}_k, \boldsymbol{p}_l)$ and $V(\boldsymbol{q}_i, \boldsymbol{q}_j, \boldsymbol{q}_k, \boldsymbol{q}_l)$. These volumes are easy to compute and are independent of $x \in P$. Two views of the same injective deformation of the teapot are shown.
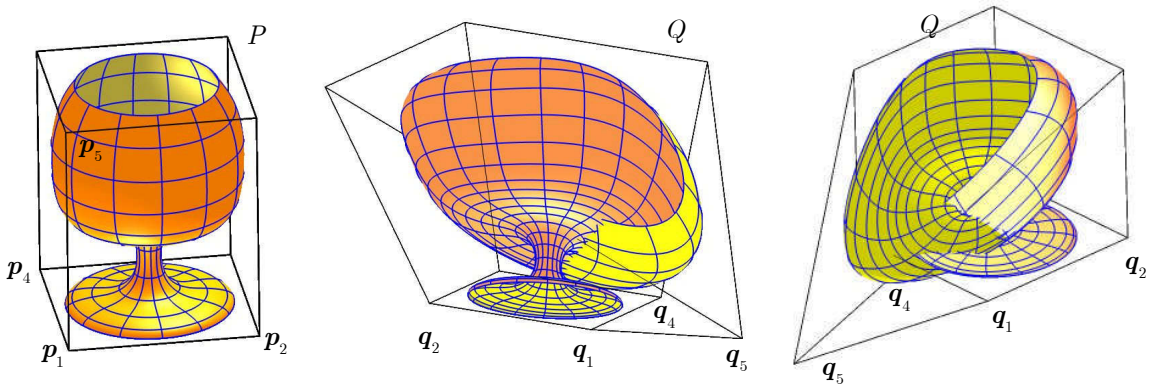
Fig. 2: Conditions of Theorem 5.2 are violated. Volumes $V(p_1, p_2, p_4, p_5)$ and $V(q_1, q_2, q_4, q_5)$ have opposite signs, which might cause undesirable self-intersections. Two views of the same setting are shown.
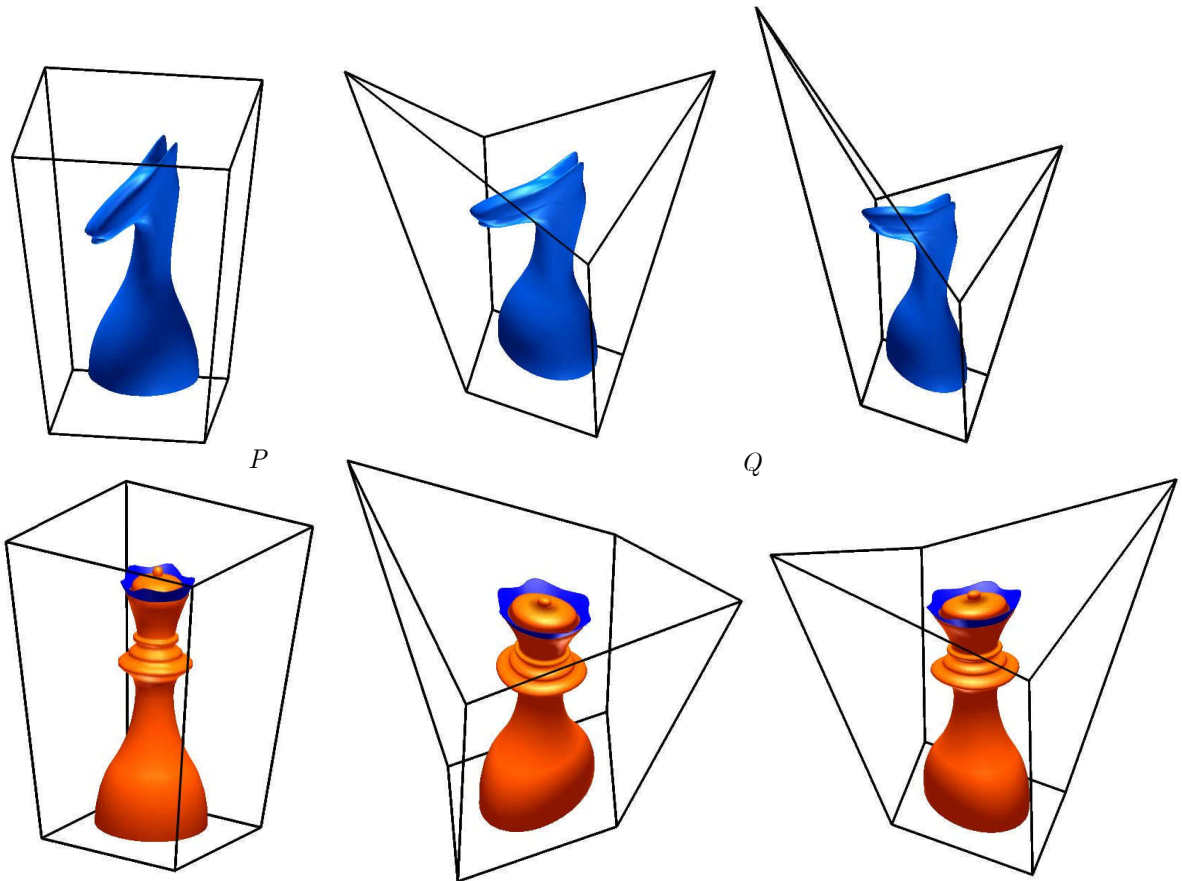

Fig. 3: Injective deformation of models of chess pieces. A knight and a queen are enclosed by a truncated pyramid P (left). Two different cube-like deformations of the knight and one deformation of the queen, displayed from two different viewports, are shown.
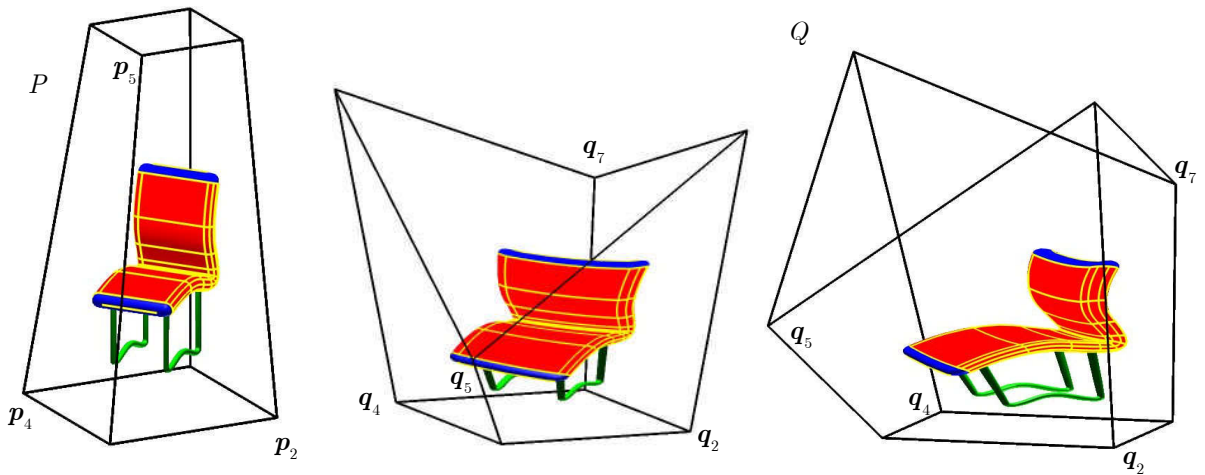
p_7

Fig. 4: Injective deformation using cube-like cages: A free-form model of a chair is enclosed in a convex polyhedron P (left). Whereas all faces of P are required to be planar quadrilaterals, faces of Q are allowed to be non-planar. The match in signs of volumes for all corresponding tetrahedrons, i.e. $V(\boldsymbol{p}_i, \boldsymbol{p}_j, \boldsymbol{p}_k, \boldsymbol{p}_l)$ and $V(\boldsymbol{q}_i, \boldsymbol{q}_j, \boldsymbol{q}_k, \boldsymbol{q}_l)$, guarantees the injectivity of the mapping.
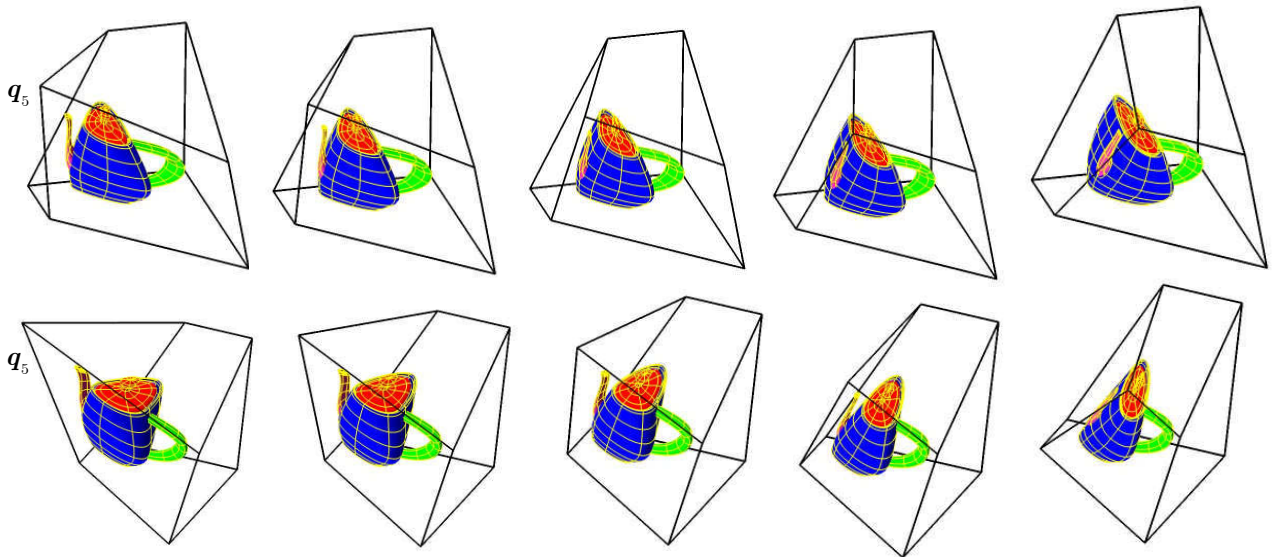

Fig. 5: Five frames of a teapot deformation from two different viewports (upper/lower row) are depicted. The cages are shown as well. Vertex $\boldsymbol{q}_5$ is moved toward the center of the cage, inducing the corresponding deformation of the teapot. The deformation is guaranteed to be injective (first four frames), whilst in the last figures (right) the sufficient conditions of Theorem 5.2 are violated.
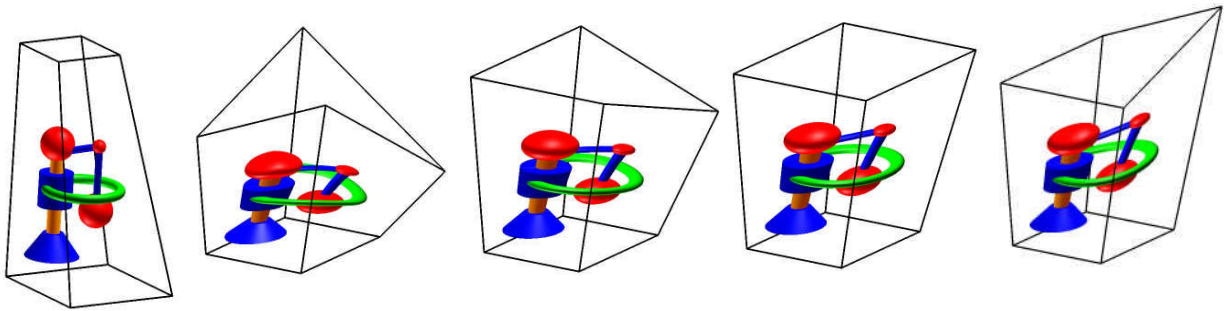
Fig. 6: Injective deformation using cube-like cages: A free-form model of a toy-robot in highly sensitive self-intersection configuration is enclosed in a convex polyhedron P (left). A self intersection free deformation is fully controlled by the match in signs of volumes for all corresponding tetrahedrons, i.e. $V(\boldsymbol{p}_i,\boldsymbol{p}_j,\boldsymbol{p}_k,\boldsymbol{p}_l)$ and $V(\boldsymbol{q}_i,\boldsymbol{q}_j,\boldsymbol{q}_k,\boldsymbol{q}_l)$. Four different deformations are shown.

The tests were performed on parametric free-form surfaces. However, our implementation could be easily modified to handle polygonal meshes, point clouds or implicit surfaces as well. In all presented examples the input surfaces are enclosed in convex cube-like polyhedra P. Their deformations are realized by moving the vertices of P resulting in cube-like cages Q.

7   CONCLUSION AND FUTURE WORK

In this paper we presented a method for deforming shapes using cube-like cages based on Warren's coordinates for convex polyhedra. Focusing on the applicability of this type of deformations, we derived a simple set of sufficient conditions on the injectivity of the underlying barycentric mapping. These conditions admit a nice geometric interpretation and can be tested in real-time.
As a matter of future research we would like to generalize our approach to support a wider class of cages. Since Warren's coordinates are defined for convex polyhedra, one can try to use general convex cages with planar faces. However, it is a challenging task to find a simple set of sufficient and/or necessary conditions on the injectivity of general barycentric mappings induced by Warren's coordinates.

REFERENCES

[1]   Ando, T.: Totally positive matrices, Linear Algebra Appl. 90, 1987, 165-219.
[2]   Bruvoll, S.; Floater, M. S.: Transfinite mean value interpolation in general dimension, Journal of Computational and Applied Mathematics, in press.
[3]   Floater, M. S.: Mean value coordinates, Comp. Aided Geom. Design 20, 2003, 19-27.
[4]   Floater, M. S.; Kós, G.; Reimers, M.: Mean value coordinates in 3D, Comp. Aided Geom. Design 22, 2005, 623-631.
[5]   Floater, M. S.; Kosinka, J.: On the injectivity of Wachspress and mean value mappings between convex polygons, to appear in Advances in Computational Mathematics.
[6]   Gain, J.; Bechmann, D.: A survey of spatial deformation from a user-centered perspective, ACM Transactions on Graphics 27, 2008, 107:1-21.
[7]   Gain, J.; Dodgson, N.: Preventing Self-Intersection under Free-Form Deformation, IEEE Transactions on Visualization and Computer Graphics 7, 2001, 289-298.
[8]   Hormann, K.; Floater, M. S.: Mean value coordinates for arbitrary planar polygons, ACM Trans. on Graphics 25, 2006, 1424-1441.
[9]   Ju, T.; Schaefer, S.; Warren, J.; Desburn, M.: A geometric construction of coordinates for convex polyhedra using polar duals, Eurographics Symposium on Geometry Processing 2005, 181-186.
[10]   Kestelman, H.: Mappings with non-vanishing Jacobian, Amer. Math. Monthly 78, 1971, 662-663.

[11]   Lipman, Y.; Kopf, J.; Cohen-Or, D.; Levin, D.: GPU-assisted positive mean value coordinates for mesh deformation, Symposium on Geometry Processing, 2007, 117-123.
[12]   Wachspress, E. L.: A rational finite element basis, Academic Press, New York, 1975.
[13]   Warren, J.: Barycentric coordinates for convex polytopes, Adv. in Comp. Math. 6, 1996, 97-108.
[14]   Weber, O.; Ben-Chen, M.; Gotsman, C.: Complex barycentric coordinates with applications to planar shape deformation, Comput. Graph. Forum 28, 2009, 587-597.